Mechanical Systems and Signal Processing 224 (2025) 112182

Contents lists available at ScienceDirect

Mechanical Systems and Signal Processing

journal homepage: www.elsevier.com/locate/ymssp

Directional importance sampling for dynamic reliability of linear structures under non-Gaussian white noise excitation

Xuan-Yi Zhang [a,b], Mauricio A. Misraji [b], Marcos A. Valdebenito [b], Matthias G.R. Faes [b,*]

[a] National Key Laboratory of Bridge Safety and Resilience, Beijing University of Technology, Beijing 100124, China
[b] Chair for Reliability Engineering, TU Dortmund University, Leonhard-Euler-Str. 5, Dortmund 44227, Germany

ARTICLE INFO

Communicated by S. Nagarajaiah

Keywords:
Dynamic reliability
Linear structural system
Non-Gaussian white noise
Directional sampling
Importance sampling

ABSTRACT

Reliability analysis of dynamic structural systems and its implications for structural design have garnered increasing attention. Sample-based methods prove insensitive to the dimension of the probability integral. Nontheless, a substantial number of realizations is necessary for estimating small failure probabilities, resulting in time-consuming computations. Recently, the Directional Importance Sampling (DIS) was introduced for linear structural systems subjected to Gaussian loads, showcasing the ability to accurately estimate small failure probabilities with a reduced number of simulations. However, this Gaussian assumption on the load makes the method inapplicable for realistic loading scenarios as they might be of non-Gaussian nature. This contribution develops the DIS method for linear structural systems subjected to loading characterized as non-Gaussian white noise. To take the advantage of both linearity in physical space and simplicity of Gaussian space, directional importance sampling is conducted in Gaussian space and the failure probability is estimated with the aid of physical space. The information is dynamically exchanged between physical and Gaussian spaces with the aid of normal and inverse-normal transformation techniques. The whole procedure of the developed DIS method is straightforward, and it provides an explicit estimator of the failure probability. The application of the developed DIS method is presented through three examples, illustrating its accuracy and efficiency for dynamic reliability analysis.

1. Introduction

In the processes of designing or assessing a structural system, it is crucial to assess the system's reliability under stochastic loads, such as earthquake ground motions, wind loads, traffic loads and so on. Dynamic responses of structural systems exhibit stochastic behavior, posing challenges for efficient evaluation. Meanwhile, the failure probability of dynamic structural systems is typically low to ensure adequate behavior during their lifetime. These factors collectively present significant challenges in the efficient assessment of dynamic reliability.

There are roughly two approaches for dynamic reliability, i.e., analytical and simulation ones. Analytical methods are developed under specific assumptions or applicable range to enable efficient evaluations, which can be categorized into the level-crossing method [1,2], the diffusion process method [3] and the probability density evolution method (PDEM) [4,5]. The original level-crossing method can only be applied for problems with known joint probability distribution function of the response, which is difficult to obtain in practice. For practical engineering, level-crossing method is developed based on either Poisson's assumption [6]

* Corresponding author.
E-mail address: matthias.faes@tu-dortmund.de (M.G.R. Faes).

https://doi.org/10.1016/j.ymssp.2024.112182
Received 5 July 2024; Received in revised form 15 November 2024; Accepted 22 November 2024
Available online 10 December 2024

or Vanmarckes's assumption [7], both of which can only be satisfied in problems with single response. The diffusion process method is formulated upon the backward Kolmogorov equation, imposing constraints on the applicable scope to one or two degrees of freedom [8,9]. PDEM adheres to the procedure where the evolution of the probability density in a stochastic system stems from the state evolution of a physical system governed by dominant physical laws [10]. While the PDEM has demonstrated success in addressing the dynamic reliability of large structures, its application is currently confined to a limited number of random variables [11]. The substantial number of random variables encountered in practical scenarios continues to pose a significant challenge.

Another approach to dynamic reliability analysis is simulation-based methods. The most fundamental sample-based method is Monte Carlo Simulation (MCS), which is well-known for its straightforward procedure and robustness. However, MCS converges slowly as the sample size increases, making it challenging to apply for estimating small failure probabilities. To improve the efficiency, many modified methods have been proposed, including surrogate methods [12,13], Latin hypercube sampling and its variants [14,15], subset simulation and its variants [16–18], Importance Sampling (IS) [19–21], line sampling [22] and post-processing simulation method [23], and so on. With advancements in simulation methods, computational time has been dramatically reduced. However, most of these advancements have concentrated on static reliability problems, with only specific cases of dynamic reliability analysis being addressed due to the high dimensionality of random parameters and the complexity of limit states. One of the particular cases is linear structural systems under Gaussian stochastic loads, where the limit state function is described by a series of hyperplanes, allowing the application of an efficient IS scheme for estimating small failure probabilities [19]. Using the concept of Domain Decomposition, another IS scheme was deduced to decrease the computational time by taking the average among the sampled directions [24]. A directional importance sampling (DIS) method is proposed based on IS scheme [25,26], which can be efficiently applied for linear structural system under Gaussian loads comprising high dimensional uncertain input parameters (e.g., a few hundreds samples for failure probability in the level of 10^{-3} or less).

Following the line of research associated with simulation methods for linear structural systems, the objective of this contribution is to extend the applicability of DIS method to linear systems subjected to non-Gaussian white noise excitation. To take the advantage of both the linearity in physical space and well-established statistical theory for Gaussian problems, the developed DIS method adopts a strategy where samples are generated in Gaussian space, and the failure probability is estimated with the aid of linearity in the physical space. The information interchange between these two spaces is facilitated through normal and inverse-normal transformation techniques. The rest of this contribution is organized as follows. Firstly, the problem under consideration is stated in Section 2. Then, DIS method is developed, with the estimator of failure probability theoretically derived in Section 3, and a directional importance sampling developed in Section 4. The application of the developed DIS method is investigated in Section 5 through three examples, with the loads following different kinds of non-Gaussian distributions. Finally, conclusions are drawn in Section 6.

2. Problem statement and notation

2.1. Structural system model

Consider a structural system modeled as linear, elastic and with classical damping subjected to stochastic loading $\mathbf{F}(t)$. The model possesses n_D degrees-of-freedom and it is assumed that its structural matrices are deterministic. The equation of motion is formulated as [27]:

$$\mathbf{M}\ddot{\mathbf{x}}(t) + \mathbf{C}\dot{\mathbf{x}}(t) + \mathbf{K}\mathbf{x}(t) = \mathbf{F}(t), \tag{1}$$

where $\ddot{\mathbf{x}}(t)$, $\dot{\mathbf{x}}(t)$, and $\mathbf{x}(t)$ are the vectors of acceleration, velocity and displacement, respectively, of dimension $n_D \times 1$; $\mathbf{M}$, $\mathbf{C}$, and $\mathbf{K}$ are the mass, damping and stiffness matrices, respectively, of dimension $n_D \times n_D$; and $\mathbf{F}(t)$ is the $(n_D \times 1)$-dimensional external excitation vector. Without loss of generality, it is assumed that the structure is at rest at the initial time, that is $\mathbf{x}(0) = \dot{\mathbf{x}}(0) = 0$.

2.2. Stochastic loading

The type of stochastic loading considered here is modeled as a non-Gaussian, band-limited white noise process, denoted by $p(t)$. The external excitation $\mathbf{F}(t)$ is then expressed as follows:

$$\mathbf{F}(t) = \mathbf{q}p(t), \tag{2}$$

where $\mathbf{q}$ is a time-independent $(n_D \times 1)$ vector that couples $p(t)$ with the corresponding degrees-of-freedom of the structure, to describe the influence of $p(t)$ on each degree-of-freedom.

While idealized white noise cannot exist in a strict mean square sense due to infinite variance, band-limited white noise offers a practical approximation that provides excitation over a finite frequency range. The non-Gaussian white noise model has seen increasing application across various fields [28–31]. In our study, the non-Gaussian nature of $p(t)$ provides an advancement over earlier studies [25,26], although the white noise assumption implies no temporal correlation within $p(t)$. This work thus offers a generalized framework that may be further refined to match the dynamics and physical properties of specific systems.

The dynamic load $p(t)$ of a duration T can be described as a discrete process $\mathbf{p}$ of a dimension n_t, with T divided by time discretization Δt, such that $n_t = T/\Delta t + 1$. Using the inverse-normal transformation, $\mathbf{p}$ can be represented as follows:

$$\mathbf{p} = F_{\mathbf{P}}^{-1}[\Phi_{\mathbf{U}}(\mathbf{u})], \tag{3}$$

where $\mathbf{u}$ is a column vector of independent standard Gaussian random variables of a dimension n_T; and $F_{\mathbf{P}}(\cdot)$ and $\Phi_{\mathbf{U}}(\cdot)$ are the cumulative distribution functions (CDFs) associated with $\mathbf{p}$ and $\mathbf{u}$, respectively. Under the assumption that $p(t)$ is non-Gaussian white noise, $F_{\mathbf{P}}(\cdot)$ can be constructed as follows:

$$F_{\mathbf{P}}(\mathbf{p}) = \prod_{k=1}^{n_t} F_{p_k}(p_k), \tag{4}$$

where $F_{p_k}(p_k)$ is the CDF of the kth element in $\mathbf{p}$, corresponding to $p(t_k)$. When the distribution of $\mathbf{p}$ is known, $F_{p_k}(p_k)$ can be directly constructed. When the distribution of $\mathbf{p}$ is unknown, the statistical moments of $\mathbf{p}$ can be applied to simulate $F_{p_k}(p_k)$ [32]. It is important to note that, Eq. (4) applies exclusively to white noise excitation. For general stochastic processes, correlation structures in $\mathbf{p}$ needs to be considered, making the construction of $F_{\mathbf{P}}(\cdot)$ significantly more complicated.

2.3. Structural response

In practice, there may be n_η responses of interest. Taking the advantage of linearity, the dynamic responses, denoted as $\eta_i(t, \mathbf{p})$, $i = 1, \ldots, n_\eta$, can be calculated as follows [33]:

$$\eta_i(t, \mathbf{p}) = \int_0^t h_i(t-\tau) p(\tau) d\tau, \tag{5}$$

where $h_i(\cdot)$ is the unit impulse response function corresponding to the ith response $\eta_i(t, \mathbf{p})$. For the particular case where $\eta_i(t, \mathbf{p})$ is a linear combination of the components of the displacement vector, $h_i(\cdot)$ can be formulated as

$$h_i(t) = \sum_{v=1}^{n_D} \frac{\boldsymbol{\gamma}_i^T \boldsymbol{\phi}_v \boldsymbol{\phi}_v^T \mathbf{q}}{\boldsymbol{\phi}_v^T \mathbf{M} \boldsymbol{\phi}_v} \frac{1}{w_{d,v}} e^{-\zeta_v w_v t} \sin(w_{d,v} t), \tag{6}$$

where $\boldsymbol{\gamma}_i$ is a constant vector; $\boldsymbol{\phi}_v$ is the vth eigenvector associated with the eigenproblem of the undamped equation of motion; w_v is the vth natural frequency of the system; ζ_v is the vth corresponding damping ratio; and $w_{d,v} = w_v\sqrt{1-\zeta_v^2}$ is the vth damped frequency.

In practical applications, $\eta_i(t, \mathbf{p})$ is often solved considering discrete time steps by an appropriate numerical integration scheme and expressed as follows:

$$\begin{aligned} \eta_i(t_k, \mathbf{p}) &= \sum_{l=1}^{k} \Delta t \epsilon_l h_i(t_k - t_l) p(t_l) \\ &= \mathbf{h}_i(t_k)\mathbf{p}, \end{aligned} \tag{7}$$

where $\mathbf{h}_i(t_k)$ is a $(1 \times n_t)$-dimensional vector evaluated at t_k, with the lth element of $\mathbf{h}_i(t_k)$ set to be $\Delta t \epsilon_l h_i(t_k - t_l)$ for $l \le k$ and 0 for $l > k$. In this study, ϵ_l is chosen according to the trapezoidal integration rule [34], yielding $\epsilon_l = 1/2$ if $l = 1$ or $l = k$; otherwise $\epsilon_l = 1$.

2.4. Failure events

For practical design purposes, the response must remain within the prescribed threshold. Accordingly, the elementary failure event at instant t_k corresponding to the ith response, denoted by $F_{i,k}$, is defined as

$$F_{i,k} = F_{i,k,1} \bigcup F_{i,k,2}, \tag{8}$$

where $F_{i,k,1}$ and $F_{i,k,2}$ are the upper and lower excursions at instant t_k corresponding to the ith response, respectively, which are mutually exclusive and defined as follows:

$$F_{i,k,1} = \{\mathbf{p} \in \Omega_{\mathbf{p}} : G_{i,1}(t_k, \mathbf{p}) \le 0\}, \quad F_{i,k,2} = \{\mathbf{p} \in \Omega_{\mathbf{p}} : G_{i,2}(t_k, \mathbf{p}) \le 0\}, \tag{9}$$

$$G_{i,1}(t_k, \mathbf{p}) = b_{i,1} - \eta_i(t_k, \mathbf{p}), \quad G_{i,2}(t_k, \mathbf{p}) = \eta_i(t_k, \mathbf{p}) - b_{i,2}, \tag{10}$$

where $G_{i,1}(t_k, \mathbf{p})$ and $G_{i,2}(t_k, \mathbf{p})$ are the performance functions corresponding to upper and lower excursions, respectively, at time t_k; $b_{i,1}$ and $b_{i,2}$ are the prescribed thresholds for upper and lower excursions considering the ith response, respectively; and $\Omega_{\mathbf{p}}$ is the domain of $\mathbf{p}$.

The structural failure within the time interval $[0, T]$, denoted by F, is the union of all the elementary failure events $F_{i,k,s}$. Based on Eq. (8), F is defined as

$$F = \bigcup_{i=1}^{n_\eta} \bigcup_{k=1}^{n_t} F_{i,k} = \bigcup_{i=1}^{n_\eta} \bigcup_{k=1}^{n_t} \bigcup_{s=1}^{2} F_{i,k,s}, \tag{11}$$

3. Estimator of failure probability with non-Gaussian loading

Failure probability P_f is the probability of the occurrence of F. Based on Eqs. (9)–(11), P_f is formulated as:

$$P_f = \text{Prob}[\exists(i \in [1, n_\eta], k \in [1, n_t], s \in [1, 2]) : G_{i,s}(t_k, \mathbf{p}) \le 0], \tag{12}$$

where Prob[·] denotes probability of the event between brackets. Generally, the threshold levels $b_{i,1}$ and $b_{i,2}$ are deterministic, and the randomness in the occurrence of F is related to $\eta_i(t_k, \mathbf{p})$. With deterministic $\mathbf{M}$, $\mathbf{C}$, and $\mathbf{K}$, $h_i(\cdot)$ has fixed form and the randomness of $\eta_i(t_k, \mathbf{p})$ comes from the stochastic loading $\mathbf{p}$. Thus, P_f is calculated as

$$P_f = \int_{\Omega_\mathbf{p}} I(\mathbf{p}) f_\mathbf{P}(\mathbf{p}) d\mathbf{p}, \tag{13}$$

where $I(\cdot)$ is an indicator function, which equals to 1 for the occurrence of F, while zero, otherwise; and $f_\mathbf{P}(\mathbf{p})$ is the joint probability density function (JPDF) of $\mathbf{p}$.

Based on Eq. (3), $f_\mathbf{P}(\mathbf{p})d\mathbf{p} = \phi_\mathbf{U}(\mathbf{u})d(\mathbf{u})$, where $\phi_\mathbf{U}(\cdot)$ is the JPDF in the n_t dimensional standard Gaussian variable space. Thus, P_f is reformulated in standard Gaussian space as follows:

$$P_f = \int_{\Omega_\mathbf{U}} I\{F_\mathbf{P}^{-1}[\Phi_\mathbf{U}(\mathbf{u})]\}\phi_\mathbf{U}(\mathbf{u})d\mathbf{u}, \tag{14}$$

where $\Omega_\mathbf{U}$ is the domain of $\mathbf{u}$.

The value of $\mathbf{u}$ can be described in terms of the unit vector in its own direction $\mathbf{u_0}$ and Euclidean norm r, namely [35]:

$$\mathbf{u} = r\mathbf{u_0}, \tag{15}$$

where $r = \|\mathbf{u}\|$; $\|\cdot\|$ denotes Euclidean norm; and $\mathbf{u_0} = \mathbf{u}/r$ is the unit vector pointing towards $\mathbf{u}$ starting from origin of the Gaussian space. Substituting Eq. (15) in Eq. (14), P_f is recast as follows:

$$P_f = \int_{\Omega_{\mathbf{U}_0}} \phi_{\mathbf{U}_0}(\mathbf{u_0}) \int_{\Omega_r} I\{F_\mathbf{P}^{-1}[\Phi_\mathbf{U}(r\mathbf{u_0})]\} f_r(r) dr d\mathbf{u_0}, \tag{16}$$

where $\Omega_{\mathbf{U}_0}$ denotes the domain of $\mathbf{u_0}$; Ω_r denotes the domain of r in the direction of $\mathbf{u_0}$; $f_r(r)$ is the PDF of r; and $\phi_{\mathbf{U}_0}(\mathbf{u_0})$ is the JPDF of $\mathbf{u_0}$.

Direct calculation of P_f based on Eq. (16) by means of simulation requires a large number of samples. To enhance the computational efficiency, an importance sampling density function is introduced, which is denoted by $f_{\mathbf{U}_0}^{IS}(\mathbf{u_0})$, and P_f is obtained as

$$P_f = \int_{\Omega_{\mathbf{U}_0}} \frac{\phi_{\mathbf{U}_0}(\mathbf{u_0})}{f_{\mathbf{U}_0}^{IS}(\mathbf{u_0})} f_{\mathbf{U}_0}^{IS}(\mathbf{u_0}) \int_{\Omega_r} I\{F_\mathbf{P}^{-1}[\Phi_\mathbf{U}(r\mathbf{u_0})]\} f_r(r) dr d\mathbf{u_0}. \tag{17}$$

Inspired by Refs. [19,36], $f_{\mathbf{U}_0}^{IS}(\mathbf{u_0})$ is defined as a weighted summation of the probability density associated with $\mathbf{u_0}$ and conditioned on the occurrence of elementary failure events as follows:

$$f_{\mathbf{U}_0}^{IS}(\mathbf{u_0}) = \sum_{i=1}^{n_\eta}\sum_{k=1}^{n_t}\sum_{s=1}^{2} w_{i,k,s} f_{\mathbf{U}_0}(\mathbf{u_0}|F_{i,k,s}), \tag{18}$$

where $w_{i,k,s}$ is the weight of $F_{i,k,s}$, which is calculated as follows:

$$w_{i,k,s} = \frac{P_{f,i,k,s}}{\hat{P}_f}, \quad \hat{P}_f = \sum_{i=1}^{n_\eta}\sum_{k=1}^{n_t}\sum_{s=1}^{2} P_{f,i,k,s}, \tag{19}$$

where $P_{f,i,k,s}$ is the failure probability corresponding to $F_{i,k,s}$. Based on the Bayes' theorem, $f_{\mathbf{U}_0}(\mathbf{u_0}|F_{i,k,s})$ is expressed as [19]

$$f_{\mathbf{U}_0}(\mathbf{u_0}|F_{i,k,s}) = \frac{\phi_{\mathbf{U}_0}(\mathbf{u_0})\text{Prob}[F_{i,k,s}|\mathbf{u_0}]}{P_{f,i,k,s}}. \tag{20}$$

Substitution of Eqs. (18)–(20) into Eq. (17) allows to reformulate the expression of P_f as follows:

$$P_f = \hat{P}_f \int_{\Omega_{\mathbf{U}_0}} f_{\mathbf{U}_0}^{IS}(\mathbf{u_0}) \int_{\Omega_r} \frac{I\{F_\mathbf{P}^{-1}[\Phi_\mathbf{U}(r\mathbf{u_0})]\}}{\sum_{i=1}^{n_\eta}\sum_{k=1}^{n_t}\sum_{s=1}^{2}\text{Prob}[F_{i,k,s}|\mathbf{u_0}]} f_r(r) dr d\mathbf{u_0}, \tag{21}$$

Note that as r^2 follows a Chi-square distribution of n_t degree-of-freedom for any $\mathbf{u_0}$ [37], and by solving the inner integral of Eq. (21), P_f can be recast as

$$P_f = \hat{P}_f \int_{\Omega_{\mathbf{U}_0}} \frac{1 - \chi_{n_t}\left(r_{min}^2\right)}{\sum_{i=1}^{n_\eta}\sum_{k=1}^{n_t}\sum_{s=1}^{2}\left[1 - \chi_{n_t}\left(r_{i,k,s}^2\right)\right]} f_{\mathbf{U}_0}^{IS}(\mathbf{u_0}) d\mathbf{u_0}, \tag{22}$$

where $\chi_{n_t}(\cdot)$ denotes the CDF of Chi-square distribution of n_t degree-of-freedom; $r_{i,k,s}$ is the Euclidean norm of $\mathbf{u}$ that makes $F_{i,k,s}$ occur in the direction of $\mathbf{u_0}$; and r_{min} is the minimum value of all $r_{i,k,s}$. Based on Eq. (22), the estimator for P_f in the developed DIS method is given as

$$P_f^{DIS} = \frac{\hat{P}_f}{N_{DIS}} \sum_{j=1}^{N_{DIS}} \theta\left(\mathbf{u_0}^{(j)}\right), \tag{23}$$

$$\theta\left(\mathbf{u}_{\mathbf{0}}^{(j)}\right)=\frac{1-\chi_{n_t}\left[\left(r_{min}^{(j)}\right)^2\right]}{\sum_{i=1}^{n_\eta}\sum_{k=1}^{n_t}\sum_{s=1}^{2}1-\chi_{n_t}\left[\left(r_{i,k,s}^{(j)}\right)^2\right]}, \tag{24}$$

where N_{DIS} is the number of samples generated in DIS; $\mathbf{u}_{\mathbf{0}}^{(j)}$ is the jth direction vectors generated according to $f_{\mathbf{U_0}}^{IS}(\mathbf{u_0})$; $r_{i,k,s}^{(j)}$ is the jth Euclidean distances of $\mathbf{u}$ that makes $F_{i,k,s}$ occur; and $r_{min}^{(j)}$ is the minimum values of all $r_{i,k,s}^{(j)}$. The level of precision of the estimated failure probability can be quantified using the coefficient of variation (COV) [38]. Based on the theoretical definition, the COV of P_f^{DIS}, denoted as COV_{DIS}, is computed as

$$COV_{DIS}=\frac{1}{P_f^{DIS}}\sqrt{\frac{1}{N_{DIS}(N_{DIS}-1)}\sum_{j=1}^{N_{DIS}}\left[\hat{P}_f\theta\left(\mathbf{u}_{\mathbf{0}}^{(j)}\right)-P_f^{DIS}\right]^2}. \tag{25}$$

As given in Eqs. (23) and (24), the estimator of failure probability developed in DIS method is similar as that of the original DIS method [26], while the evaluation of failure probabilities and weights corresponding to upper and lower excursions are conducted separately. There are three tasks for estimating the failure probability: (1) evaluation of the elementary failure probability $P_{f,i,k,s}$; (2) generation of the direction vector samples $\mathbf{u}_{\mathbf{0}}^{(j)}$, following the importance sampling density function $f_{\mathbf{U_0}}^{IS}(\mathbf{u_0})$; and (3) estimation of the Euclidean norms associated with the occurrence of elementary failure events, i.e., $r_{i,k,s}^{(j)}$. For non-Gaussian problems, the LSFs in Gaussian space may be non-linear and the existing DIS procedure [26] cannot be applied directly. In the following, a numerical implementation procedure is proposed to cope with the case where $\mathbf{p}$ is modeled as weakly non-Gaussian white noise excitation.

4. Practical implementation with non-Gaussian white noise excitation

4.1. Evaluation of elementary failure probability

The elementary failure events as described in Eqs. (9) and (10) can be seen as time-independent failure events, and the corresponding elementary failure probabilities $P_{f,i,k,s}$ can be easily calculated using classical time-independent reliability methods, such as the first-order reliability method (FORM) [37] and method of moments [32,39]. Generally, the choice of reliability analysis method could be made based on the linearity and dimensionality of LSFs in Gaussian space. When the LSFs in Gaussian space is slightly non-linear, FORM can be applied, while the method of moments should be utilized otherwise. For a linear structural system under white noise excitation, the response given in Eq. (7) is a summation of a large number of independent random variables. This results in the response exhibiting slightly non-Gaussian characteristics, allowing the method of moments to be accurately and efficiently applied. Thus, in this study, the method of moments is applied for computing $P_{f,i,k,s}$.

The basic idea for the method of moments is to simulate the distributions of the performance function based on its statistical moments, and the failure probability is defined as the value of the CDF of the performance function at zero. In this paper, the cubic normal distribution [40], is applied to simulate the distributions of performance functions, since experience shows that it is sufficiently flexible to reflect the statistical information, and $P_{f,i,k,s}$ can be defined as follows:

$$P_{f,i,k,s}=F_{G_{i,k,s}}(0)=\Phi(u_{i,k,s}), \tag{26}$$

where $F_{G_{i,k,s}}(\cdot)$ is the CDF of elementary performance function $G_{i,s}(t_k,\mathbf{p})$; and $u_{i,k,s}$ is the equivalent Gaussian random variables transforming from 0 and expressed as [41]:

$$u_{i,k,s}=\frac{\sqrt[3]{2}m}{\sqrt[3]{\Delta-q}}-\frac{\sqrt[3]{\Delta-q}}{\sqrt[3]{2}}+\frac{a_3}{3a_4}, \tag{27}$$

$$\Delta=\sqrt{q^2+4m^3}, \tag{28}$$

$$m=\frac{3a_2a_4-a_3^2}{9a_4^2},\quad q=\frac{2a_3^3-9a_2a_3a_4-27a_4^2(a_2+\kappa\mu/\sigma)}{27a_4^3}, \tag{29}$$

where μ and σ are the mean and standard deviations of the performance function, respectively; and a_2, a_3, a_4 and κ are the parameters and calculated as follows [42]:

$$a_0=\frac{\sqrt{3\alpha_4-4\alpha_3^2-5}-2}{1-(3\alpha_3^2+1)/\alpha_4^2}, \tag{30}$$

$$a_2=1-3a_4,\quad a_3=\frac{5+(35-\alpha_4^2)a_4^2}{9a_0+30-0.8\alpha_3^2}\alpha_3, \tag{31}$$

$$a_4=\frac{2a_0}{2a_0+46(1-1/\alpha_4^2)-\alpha_3^2},\quad \kappa=\frac{1}{\sqrt{1+2a_3^2+6a_4^2}}, \tag{32}$$

where α_3 and α_4 are the skewness and kurtosis of performance function, respectively. When α_3 and α_4 fall outside the range of Eqs. (27)–(29), a complete expression of $u_{i,k,s}$ is required [41].

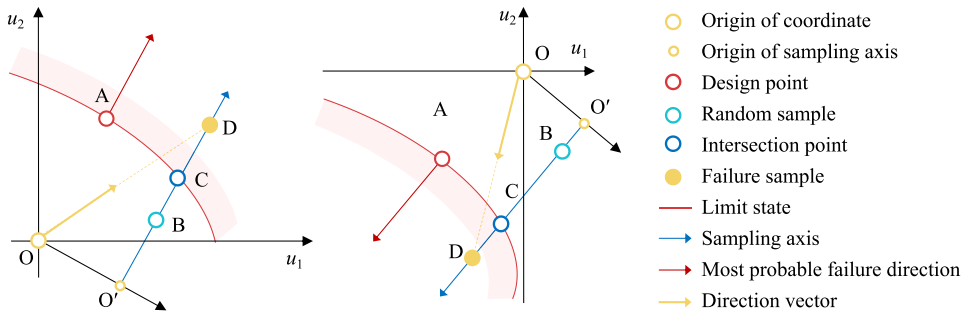

Fig. 1. Directional importance sampling in DIS method.

Based on Eq. (10), the first four moments of performance function can be easily determined based on those of the responses. As the performance functions for upper and lower excursions are different, the moment evaluation formulas are also different as follows:

$$\text{Upper excursion}: \quad \mu = b_{i,1} - \mu_{\eta_i}(t_k), \sigma = \sigma_{\eta_i}(t_k), \alpha_3 = -\alpha_{3\eta_i}(t_k), \alpha_4 = \alpha_{4\eta_i}(t_k), \tag{33}$$

$$\text{Lower excursion}: \quad \mu = \mu_{\eta_i}(t_k) - b_{i,2}, \sigma = \sigma_{\eta_i}(t_k), \alpha_3 = \alpha_{3\eta_i}(t_k), \alpha_4 = \alpha_{4\eta_i}(t_k), \tag{34}$$

where $\mu_{\eta_i}(t_k), \sigma_{\eta_i}(t_k), \alpha_{3\eta_i}(t_k), \alpha_{4\eta_i}(t_k)$ are the mean, standard deviation, skewness and kurtosis of the ith response at instant t_k, respectively. Based on Eq. (7), the moments of response can be calculated as follows:

$$\mu_{\eta_i}(t_k) = \mathbf{h}_i(t_k)\boldsymbol{\mu}_{\mathbf{P}}, \tag{35}$$

$$\sigma_{\eta_i}(t_k) = \sqrt{[\mathbf{h}_i(t_k)]^{\circ 2}\boldsymbol{\sigma}_{\mathbf{P}}^{\circ 2}}, \tag{36}$$

$$\alpha_{3\eta_i}(t_k) = \frac{[\mathbf{h}_i(t_k)]^{\circ 3}\boldsymbol{\alpha}_{\mathbf{3P}}\boldsymbol{\sigma}_{\mathbf{P}}^{\circ 3}}{\sigma_{\eta_i}^3(t_k)}, \tag{37}$$

$$\alpha_{4\eta_i}(t_k) = \frac{[\mathbf{h}_i(t_k)]^{\circ 4}\boldsymbol{\alpha}_{\mathbf{4P}}\boldsymbol{\sigma}_{\mathbf{P}}^4}{\sigma_{\eta_i}^4(t_k)} + \frac{3\{\mathbf{D}[\mathbf{h}_i(t_k)^T]^{\circ 2}[\mathbf{h}_i(t_k)]^{\circ 2} - [\mathbf{h}_i(t_k)]^{\circ 4}\}\boldsymbol{\sigma}_{\mathbf{P}}^{\circ 4}}{\sigma_{\eta_i}^4(t_k)}, \tag{38}$$

where $\boldsymbol{\mu}_{\mathbf{P}}$ and $\boldsymbol{\sigma}_{\mathbf{P}}$ are n_T-dimensional column vectors of mean value and standard deviation of $\mathbf{P}$, respectively; $\boldsymbol{\alpha}_{\mathbf{3P}}$ and $\boldsymbol{\alpha}_{\mathbf{4P}}$ are $(n_T \times n_T)$-dimensional diagonal matrices with the diagonal set to be the skewness and kurtosis of $\mathbf{P}$, respectively; $\mathbf{D}$ is a $(1 \times n_T)$-dimensional vector of ones; and $(\cdot)^{\circ x}$ denotes the Hadamard power x of the argument.

4.2. Generation of direction vector sample

4.2.1. Expression of direction vector

The importance sampling density function, as given in Eq. (18), is defined as the summation of weighted conditional distributions. Thus, direction vector samples following the importance sampling density function can be generated following two steps: first, an elementary failure event is selected based on the corresponding weight, which can be directly obtained as given in Eq. (19); and second, the direction vector sample is generated conditioned on the occurrence of selected failure event, which will be discussed in the following.

The direction vector is an unit vector pointing to a failure sample generated, which is in the failure domain of the selected failure event. Then, the direction vector is defined based on the failure sample as follows:

$$\mathbf{u}_{\mathbf{0}}^{(j)} = \frac{\mathbf{u}_{\mathbf{F}}^{(j)}}{\|\mathbf{u}_{\mathbf{F}}^{(j)}\|}, \tag{39}$$

where $\mathbf{u}_{\mathbf{F}}^{(j)}$ is the coordinate of the jth failure sample. Based on Eq. (39), to determine the direction vector, a failure sample should be generated. In this study, the failure sample is obtained by modifying a random sample to fall within the failure domain of the selected failure event. As the LSFs in Gaussian space reflect not only the physical definition of failure but also the statistical information of stochastic loads and their effect over the structural response, the failure sample is generated in Gaussian space. To facilitate this modification, the most probable modification direction needs to be defined first, which should provide the shortest distance from the random sample to the failure domain. For practical implementation, the modification direction for different random samples is approximated as the most probable failure direction at the design point. In this study, the design point is searched using the Hasofer–Lind–Rackwitz–Fiessler (HLRF) algorithm [43], and the detailed procedure for identifying the design point can be found in Appendix.

To describe the sample generation procedure clearly, a schematic graph is depicted in Fig. 1, where u_1 and u_2 represent the loads at different instants in Gaussian space. First, the design point A is identified to determine the most probable failure direction. Then,

a random sample point B is generated. Next, a sampling axis is constructed, defined as the line along the most probable failure direction that passes through the random sample point. Fourth, the random sample point B is modified to fall within the failure domain by adding a modification vector $\overrightarrow{BD}$, which is aligned with the sampling axis, resulting in the failure sample point D. Note that the length of the modification vector, $\|\overrightarrow{BD}\|$, is randomly generated. Given that $\overrightarrow{OD} = \overrightarrow{OB} + \overrightarrow{BD}$, where point O is the origin, the failure sample D can be expressed as follows:

$$\mathbf{u}_{\mathbf{F}}^{(j)} = \mathbf{u}_{\mathbf{R}}^{(j)} + \alpha^{(j)}\mathbf{d}_{i,k,s}, \tag{40}$$

where $\mathbf{u}_{\mathbf{R}}^{(j)}$ is the value of jth random sample; $\alpha^{(j)}$ is defined as the modification coefficient, which represents the length of the modification vector $\overrightarrow{BD}$; and $\mathbf{d}_{i,k,s}$ is the unit vector in the most probable failure direction of the elementary failure event $F_{i,k,s}$. $\mathbf{u}_{\mathbf{R}}^{(j)}$ can be sampled following standard Gaussian distribution (with no conditions). Based on the definition, $\mathbf{d}_{i,k,s}$ is the unit normal vector of $G_{i,s}(t_k, \mathbf{p})$ at the design point and can be calculated as

$$\mathbf{d}_{i,k,s} = \frac{\mathbf{u}_{i,k,s}^{*}}{\|\mathbf{u}_{i,k,s}^{*}\|}, \tag{41}$$

where $\mathbf{u}_{i,k,s}^{*}$ is the design point corresponding to $G_{i,s}(t_k, \mathbf{p})$. In practice, $\mathbf{u}_{i,k,s}^{*}$ can be obtained using HLRF algorithm [37] (details can be seen in Appendix). The generation of modification coefficients $\alpha^{(j)}$ will be discussed in the following.

4.2.2. Generation of modify coefficient

Consider that $\|\overrightarrow{BD}\| = \|\overrightarrow{BC}\| + \|\overrightarrow{CD}\|$, where point C is the intersection of the limit state hypersurface and the sampling axis, $\alpha^{(j)}$ can be calculated as follows:

$$\alpha^{(j)} = \alpha_R^{(j)} + \alpha_F^{(j)}, \tag{42}$$

where $\alpha_R^{(j)}$ and $\alpha_F^{(j)}$ represent the lengths of $\overrightarrow{BC}$ and $\overrightarrow{CD}$, respectively. To generate $\alpha^{(j)}$, the values of $\alpha_R^{(j)}$ and $\alpha_F^{(j)}$ need to be obtained.

(1) Computation of $\alpha_R^{(j)}$. As the coordinate of point C equals to $\overrightarrow{BC}$ plus the coordinate of point B, the coordinates of point C, denoted as $\mathbf{u}_{\mathbf{L}}$, is a formula of $\alpha_R^{(j)}$ as follows:

$$\mathbf{u}_{\mathbf{L}} = \mathbf{u}_{\mathbf{R}}^{(j)} + \alpha_R^{(j)}\mathbf{d}_{i,k,s}, \tag{43}$$

Given that point C is on the limit state surface, $\alpha_R^{(j)}$ can be obtained by solving the following equation:

$$G_{U,i,s}(t_k, \mathbf{u}_{\mathbf{L}}) = 0, \tag{44}$$

where $G_{U,i,s}(\cdot,\cdot)$ is the performance function in Gaussian space, which is constructed by substituting Eq. (3) into Eq. (10) as follows:

$$G_{U,i,1}(t_k, \mathbf{u}) = b_{i,1} - \eta_i(t_k, F_{\mathbf{P}}^{-1}[\Phi_{\mathbf{U}}(\mathbf{u})]), \quad G_{U,i,2}(t_k, \mathbf{u}) = \eta_i(t_k, F_{\mathbf{P}}^{-1}[\Phi_{\mathbf{U}}(\mathbf{u})]) - b_{i,2}. \tag{45}$$

Since the inverse normal transformation given in Eq. (3) is nonlinear for non-Gaussian $\mathbf{p}$, finding an analytical solution to Eq. (44) is not possible. As an alternative, $\alpha_R^{(j)}$ can be obtained by finding the minimum value of $\|G_{U,i,s}(t_k, \mathbf{u}_{\mathbf{L}})\|$ using optimization algorithms, such as sequential quadratic programming. Numerical tests show that such an optimization algorithm can converge within 5 iterations for a linear structural system under weakly non-Gaussian white noise excitation.

(2) Generation of $\alpha_F^{(j)}$. Given that $\|\overrightarrow{CD}\| = \|\overrightarrow{O'D}\| - \|\overrightarrow{O'C}\|$, where point O' is the origin of sampling axis, $\alpha_F^{(j)}$ is calculated as

$$\alpha_F^{(j)} = \beta_F^{(j)} - \beta_L^{(j)}, \tag{46}$$

where $\beta_F^{(j)}$ and $\beta_L^{(j)}$ are the lengths of $\overrightarrow{O'D}$ and $\overrightarrow{O'C}$, respectively. As $\overrightarrow{O'C}$ is the projection of $\overrightarrow{OC}$ on the sampling axis, $\beta_L^{(j)}$ is calculated as follows:

$$\beta_L^{(j)} = |\mathbf{u}_{\mathbf{L}}^{T}\mathbf{d}_{i,k,s}|, \tag{47}$$

To take the advantage of the rotational invariant character of Gaussian space [37], point D is interpreted as the sample along the sampling axis and follows standard normal distribution. Furthermore, to ensure the failure sample D exist within the failure domain, $\|\overrightarrow{O'D}\|$ should be larger than $\|\overrightarrow{O'C}\|$. Then, $\beta_F^{(j)}$ is generated as follows:

$$\beta_F^{(j)} = -\Phi^{-1}[\gamma^{(j)}\Phi(-\beta_L^{(j)})], \tag{48}$$

where $\gamma^{(j)}$ is the jth sample generated following uniform distribution within the range of [0,1].

4.2.3. Procedure of direction vector sampling

The steps to generate direction vector samples are summarized in Fig. 3, and details are discussed as follows.

(1) Generate a pair of $\{i, k, s\}$ based on the weights $w_{i,k,s}$.
(2) Identify the design point $\mathbf{u}_{i,k,s}^{*}$, corresponding to the selected elementary failure event.
(3) Define the unit vector associated with most probable failure direction $\mathbf{d}_{i,k,s}$, with the aid of Eq. (41).
(4) Generate a random sample $\mathbf{u}_{\mathbf{R}}^{(j)}$ in Gaussian space.

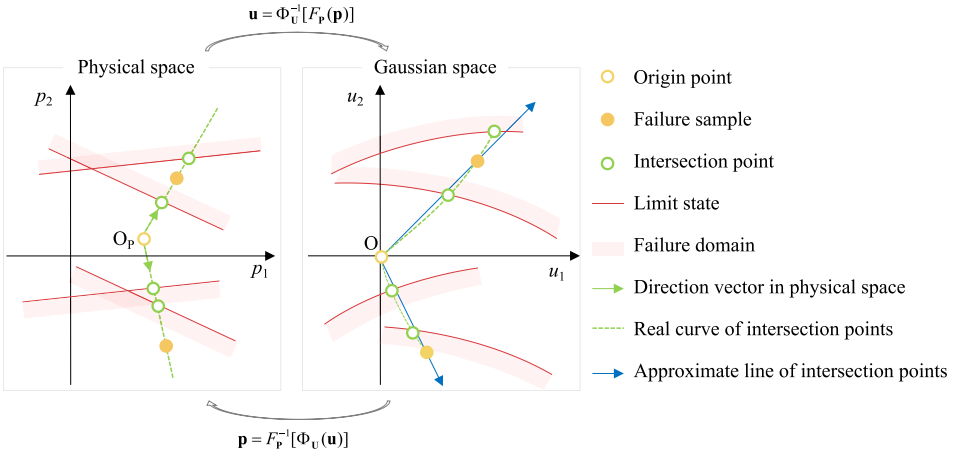

Fig. 2. Approximation of direction vector in DIS method.

(5) Generate $\alpha^{(j)}$. First, calculate $\alpha_R^{(j)}$ by solving Eqs. (43)–(45). Then, generate $\alpha_F^{(j)}$ using Eqs. (46)–(48). Finally, calculate $\alpha^{(j)}$ based on Eq. (42).
(6) Calculate $\mathbf{u}_{\mathbf{F}}^{(j)}$ based on Eq. (40).
(7) Calculate the direction vector sample $\mathbf{u}_{\mathbf{0}}^{(j)}$ based on Eq. (39).

Please note that the procedure described above performs best whenever the loading model is weakly non-Gaussian. Such behavior has been validated numerically. However, in case that the non-Gaussianity is strong, it is necessary to modify step (4), to take non-Gaussian behavior of the system along the direction which is orthogonal to that of the design point associated with the corresponding elementary failure event.

4.3. Estimation of Euclidean norms associated with the occurrence of elementary failure events

Recall that $r_{i,k,s}$ corresponds to the Euclidean distances between the origin of the standard normal space and the elementary failure domains along the ray associated with the unit vector $\mathbf{u}_{\mathbf{0}}$. These Euclidean distances are required to estimate the failure probability in Eq. (22). With the direction vector sample $\mathbf{u}_{\mathbf{0}}^{(j)}$ generated using the procedure described in Section 4.2, $\mathbf{u}$ can be expressed as $r\mathbf{u}_{\mathbf{0}}^{(j)}$. Then, $r_{i,k,s}^{(j)}$ can be obtained by solving the following equations:

$$G_{U,i,s}(t_k, r_{i,k,s}^{(j)}\mathbf{u}_{\mathbf{0}}^{(j)}) = 0. \tag{49}$$

As given in Eq. (45), $G_{U,i,k,s}(\cdot,\cdot)$ is defined based on $F_{\mathbf{P}}^{-1}(\cdot)$ and $\Phi_{\mathbf{U}}(\cdot)$, which are nonlinear and complex. In practice, direct calculation of $r_{i,k,s}^{(j)}$ in Gaussian space based on Eqs. (49) is generally challenging.

To improve the computational efficiency, $r_{i,k,s}^{(j)}$ is approximately calculated by taking the advantage of the linearity in physical space. The procedure is schematically depicted in Fig. 2, where $\{p_1, p_2\}$ and $\{u_1, u_2\}$ are the loads at two time instants in physical and Gaussian spaces, respectively.

Firstly, the failure sample and origin of Gaussian space are transformed to physical space with the aid of inverse-normal transformation as follows:

$$\mathbf{p}_{\mathbf{F}}^{(j)} = F_{\mathbf{P}}^{-1}[\Phi_{\mathbf{U}}(\mathbf{u}_{\mathbf{F}}^{(j)})], \tag{50}$$

$$\mathbf{O}_{\mathbf{P}} = F_{\mathbf{P}}^{-1}[\Phi_{\mathbf{U}}(\mathbf{0})], \tag{51}$$

where $\mathbf{p}_{\mathbf{F}}^{(j)}$ is the failure sample in physical space corresponding to $\mathbf{u}_{\mathbf{F}}^{(j)}$; and $\mathbf{O}_{\mathbf{P}}$ is the equivalent point in physical space transformed from origin of Gaussian space. Based on $\mathbf{p}_{\mathbf{F}}^{(j)}$ and $\mathbf{O}_{\mathbf{P}}$, the unit direction vector pointing to the failure sample in physical space, denoted as $\mathbf{p}_{\mathbf{0}}^{(j)}$, can be calculated as follows:

$$\mathbf{p}_{\mathbf{0}}^{(j)} = \frac{\mathbf{p}_{\mathbf{F}}^{(j)} - \mathbf{O}_{\mathbf{P}}}{\|\mathbf{p}_{\mathbf{F}}^{(j)} - \mathbf{O}_{\mathbf{P}}\|}. \tag{52}$$

Based on $\mathbf{p}_{\mathbf{0}}^{(j)}$, the set of loads $\mathbf{p}$ contained in the ray associated with $\mathbf{p}_{\mathbf{0}}^{(j)}$ can be expressed as $c\mathbf{p}_{\mathbf{0}}^{(j)}$, where c is the Euclidean norm of $\mathbf{p}$. As the performance function in physical space is linear, the value of c for the samples that first intersect the failure domain corresponding to $F_{i,k,s}$, denoted as $c_{i,k,s}^{(j)}$, can be analytically calculated as follows:

$$c_{i,k,s}^{(j)} = \frac{b_{i,s} - \eta_i(t_k, \mathbf{O}_{\mathbf{P}})}{\eta_i(t_k, \mathbf{p}_{\mathbf{0}}^{(j)})}. \tag{53}$$

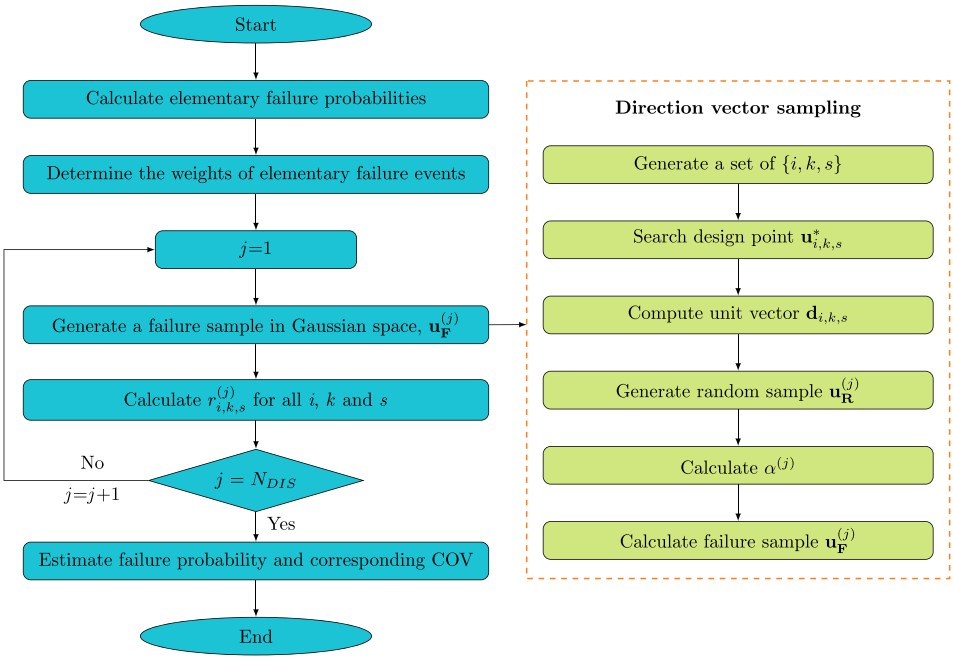

Fig. 3. Flowchart of the developed DIS method for dynamic reliability analysis.

Given the value of $c_{i,k,s}^{(j)}$, the coordinates $\mathbf{p}$ along the directions of $\mathbf{p}_{\mathbf{0}}^{(j)}$ that intersect the limit state function associated with the elementary failure domain $F_{i,k,s}$, denoted by $\mathbf{p}_{i,k,s}^{(j)}$, can be obtained as follows:

$$\mathbf{p}_{i,k,s}^{(j)} = c_{i,k,s}^{(j)} \mathbf{p}_{\mathbf{0}}^{(j)} + \mathbf{O}_{\mathbf{P}}. \tag{54}$$

Transforming $\mathbf{p}_{i,k,s}^{(j)}$ into Gaussian space gives the equivalent $\mathbf{u}$, denoted as $\mathbf{u}_{a,i,k,s}^{(j)}$, which is formulated as follows:

$$\mathbf{u}_{a,i,k,s}^{(j)} = \boldsymbol{\Phi}_{\mathbf{U}}^{-1}[F_{\mathbf{P}}(\mathbf{p}_{i,k,s}^{(j)})]. \tag{55}$$

Then, $r_{i,k,s}^{(j)}$ can be approximated as follows:

$$r_{i,k,s}^{(j)} = \|\mathbf{u}_{a,i,k,s}^{(j)}\|. \tag{56}$$

It should be noted that, the normal and inverse normal transformations based on $F_{\mathbf{P}}(\cdot)$ and $\boldsymbol{\Phi}_{\mathbf{U}}^{-1}(\cdot)$ are generally non-linear, $(r_{i,k,s}^{(j)})^2$ calculated by using Eq. (56) does not follow Chi-square distribution. The deviation from that distribution is directly linked with the degree of non-Gaussianity associated with $\mathbf{p}$. Based on numerical calculations, the non-linearity of the normal and inverse normal transformations can be neglected for weakly non-Gaussian white noise excitations with skewness less than 1.6 and kurtosis less than 8.0. And then, $(r_{i,k,s}^{(j)})^2$ can be approximately assumed to follow Chi-squared distribution of n_t degree-of-freedom. When $\mathbf{p}$ is not white noise, or when its skewness and kurtosis fall outside the applicable range, approximating $(r_{i,k,s}^{(j)})^2$ using a Chi-square distribution can lead to significant errors, necessitating further research for such cases.

4.4. Procedure of developed DIS method for dynamic reliability analysis

As discussed above, DIS method is developed for problems under weakly non-Gaussian white noise excitation, by taking the advantage of both linearity in physical space and rotational invariance of Gaussian space. The directional importance sampling is conducted in Gaussian space and the elementary failure probability conditioned on the sampled direction is estimated based on points detected in physical space. The vectors in different spaces are equivalently transformed based on normal and inverse normal transformation techniques. The procedure of the developed DIS method is summarized in Fig. 3, and details are discussed as follows:

(1) Calculate failure probability $P_{f,i,k,s}$ for all elementary upper and lower excursions (details can be found in Section 4.1).
(2) Determine the weights $w_{i,k,s}$ for all elementary failure events based on Eq. (19).
(3) Set $j = 1$.
(4) Generate a failure sample in Gaussian space (details can be found in Section 4.2.3).
(5) Calculate $r_{i,k,s}^{(j)}$ based on Eqs. (50)–(56) for $i = 1, \ldots, n_\eta$, $k = 1, \ldots, n_t$, and $s = 1, 2$ (details can be found in Section 4.3).
(6) In case $j = N_{DIS}$, go to step 7. Otherwise, return to step 4 with $j = j + 1$.

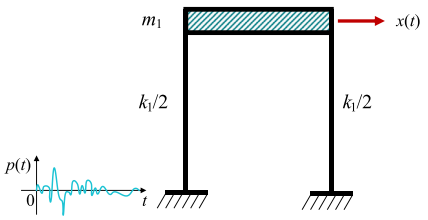

Fig. 4. Schematic graph of one-story shear beam model in example 1.

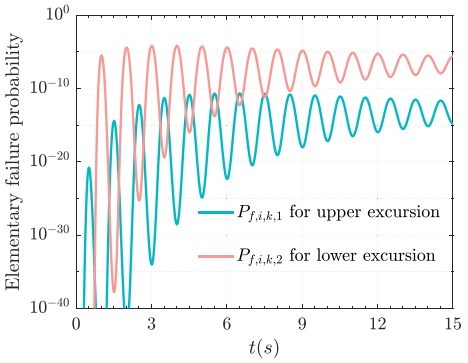

Fig. 5. Elementary failure probabilities.

(7) Estimate the failure probability based on Eqs. (23) and (24), and corresponding COV based on (25).

5. Illustrative examples

To evaluate the accuracy and efficiency of the developed DIS method, three examples are examined: a single-degree-of-freedom model, a two-degree-of-freedom model and a 20 degrees-of-freedom model. The single-degree-of-freedom oscillator, adopted from [19], is used to demonstrate the detailed procedure of the DIS method, highlighting the impacts of non-Gaussianity and failure probability. The two-degree-of-freedom model analyzes the efficiency of the DIS method to problems with multiple degrees of freedom. The third example aims to examine the application of the developed DIS method in a problem involving several degrees-of-freedom.

5.1. Example 1: Single-degree-of-freedom oscillator

The first example considers a one-story shear beam model subjected to stochastic force, as shown in Fig. 4, with the mass $m_1 = 1\,\text{kg}$, stiffness $k_1 = 4\pi^2$ N/m and damping ratio $d = 2\%$. The response of interest is the top displacement relative to the ground. The force is modeled as a discrete non-Gaussian white noise with spectral intensity $S = 1\,\text{m}^2/\text{s}^3$, duration $T = 15$ s and discrete time step $\Delta t = 0.01$ s. The standard deviation of the force, denoted by σ_P, is $\sqrt{2\pi S/\Delta t}$. The objective is to estimate the first excursion probability of the system.

5.1.1. Discussion on detailed results

To explain the detailed procedure of the developed DIS method, the load $p(t)$ is assumed to follow lognormal distribution with the coefficient of variation, denoted by COV_P, equals to 0.35. The thresholds for upper and lower excursions, i.e., $b_{1,1}$ and $b_{1,2}$, are set to be 6.0 m and −1.0 m, respectively. Based on Fig. 3, the developed DIS method can be performed. The first step is to compute the elementary failure probabilities, i.e., $P_{f,i,k,s}$, and the results are shown in Fig. 5. With $P_{f,i,k,s}$ obtained, $\hat{P}_f$ is directly calculated as 0.005, and the weights for the elementary failure events, i.e., $w_{i,k,s}$ is then obtained, as shown in Fig. 6.

The design points in Gaussian space corresponding to elementary failure events are obtained using HLRF algorithm as shown in Appendix. The next step is to generate failure samples using the procedure illustrated in Fig. 3. For illustration, the procedure for generating failure samples conditioned on the occurrence of upper excursion at $t = 0.02$ s is discussed in detail with the thresholds redefined as $b_{1,1} = 0.028$ m and $b_{1,2} = 0.006$ m. For this case, the load $\mathbf{p}$ has two components, which are denoted by p_1 and p_2. Correspondingly, the equivalent vector $\mathbf{u}$ in Gaussian space also has two components, which are denoted by u_1 and u_2. The modification of thresholds aims to enable the sample generation for a two-dimensional space, while the design points will be changed to $\mathbf{u}^*_{1,1,1} = [2.1448, 2.1595]$ and $\mathbf{u}^*_{1,1,2} = [-2.3748, -2.3840]$. With the design points defined, the unit vectors in the most probable failure direction are obtained as $\mathbf{d}_{1,1,1} = [0.7047, 0.7095]$ and $\mathbf{d}_{1,1,2} = [-0.7057, -0.7085]$, with the aid of Eq. (41). For illustration, two random

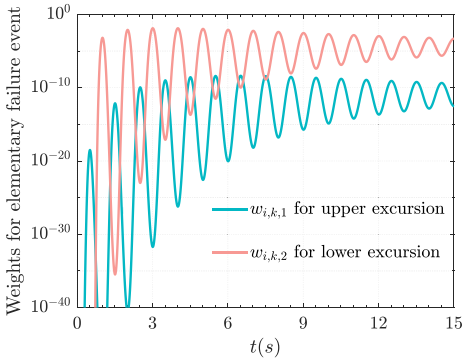

Fig. 6. Weights of elementary failure events.

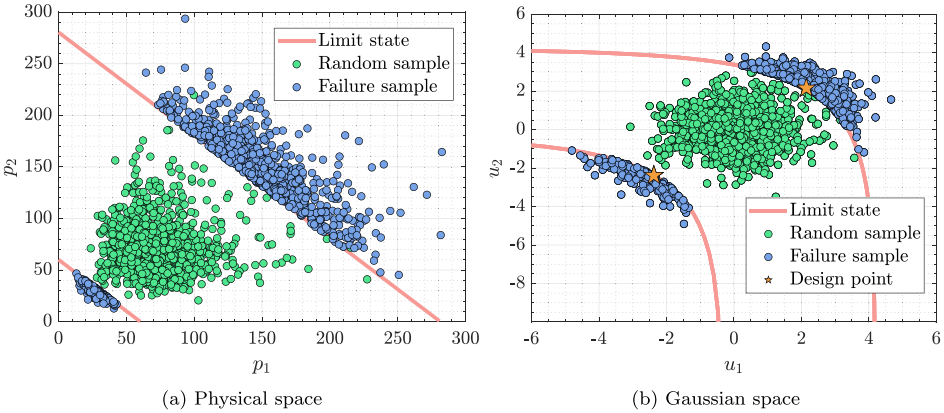

Fig. 7. Random and failure samples generated in Example 1.

samples are generated following standard Gaussian distribution for upper and lower excursions, with $\mathbf{u}_{\mathbf{R}}^{(1)} = [-1.1724, 0.5650]$ and $\mathbf{u}_{\mathbf{R}}^{(2)} = [0.5790, 0.2179]$, respectively. Based on Eq. (42), $\alpha_R^{(1)}$ and $\alpha_R^{(2)}$ can be obtained as 3.2891 and 3.9363, respectively. Then, using Eq. (46), $\alpha_F^{(1)}$ and $\alpha_F^{(2)}$ are generated as 8.43×10^{-4} and 0.6008, respectively. Based on Eq. (40), the failure sample in Gaussian space can be calculated as $\mathbf{u}_{\mathbf{F}}^{(1)} = [1.146, 2.8993]$ and $\mathbf{u}_{\mathbf{F}}^{(2)} = [-2.623, -2.9965]$. Finally, the failure samples in physical space are obtained using inverse-normal transformation given in Eq. (3) as $\mathbf{p}_{\mathbf{F}}^{(1)} = [99.7966, 181.1188]$ and $\mathbf{p}_{\mathbf{F}}^{(2)} = [27.7131, 24.4087]$. With the same procedure, $N_{DIS} = 1000$ random and failure samples can be obtained. The generated samples in physical and Gaussian spaces are depicted in Figs. 7(a) and 7(b), respectively. It is shown that the failure samples are within failure domain while close to the design points, which implies the rationality of the sampling scheme.

Following the same procedure, the failure samples for the case with $b_{1,1} = 6$ m and $b_{1,2} = -1$ m are generated. And then, the values of $r_{i,k,s}^{(j)}$ for elementary failure events can be obtained. The failure probability is estimated as 0.4982×10^{-3}. For comparison, crude MCS is also performed with 10^7 stochastic loading samples generated, and the failure probability obtained is 0.4990×10^{-3}. The failure probability obtained from the developed DIS method is close to that from MCS, with the relative error obtained as 0.16%, which shows the accuracy of the developed DIS method. The COVs of P_f obtained from DIS method with 1000 samples is around 0.18%, which shows the stability of developed DIS method.

5.1.2. *Influence of non-Gaussianity*

To investigate the influence of non-Gaussianity on the performance of the developed DIS method, dynamic reliability analysis is analyzed with $\mathrm{COV_P} = 0.25, 0.30, 0.35, 0.40, 0.45, 0.50$. The failure probabilities obtained from the developed DIS method using 1000 samples are compared with those from crude MCS in Figs. 8(a)–8(f), and the corresponding COVs of the estimated failure probabilities are compared in Figs. 9(a)–9(f). To facilitate direct comparison, dashed lines are used to extend the DIS results in Figs. 8(a)–8(f). It is illustrated that:

(1) For weakly non-Gaussian cases, i.e., $\mathrm{COV_P} \leq 0.50$, the failure probability obtained from the developed DIS method is close to that obtained using MCS. This indicates the estimator of the developed DIS method is accurate.
(2) The failure probabilities obtained by DIS method become stable with less than 1000 samples, and the COV of failure probability is lower than 0.2% with 1000 samples. In contrast, MCS requires at least 10^6 samples to stabilize. This is because the developed DIS method takes the advantage of directional and importance sampling to improve the efficiency. This results indicate the estimator of the developed DIS method convergence much quicker compared with MCS.

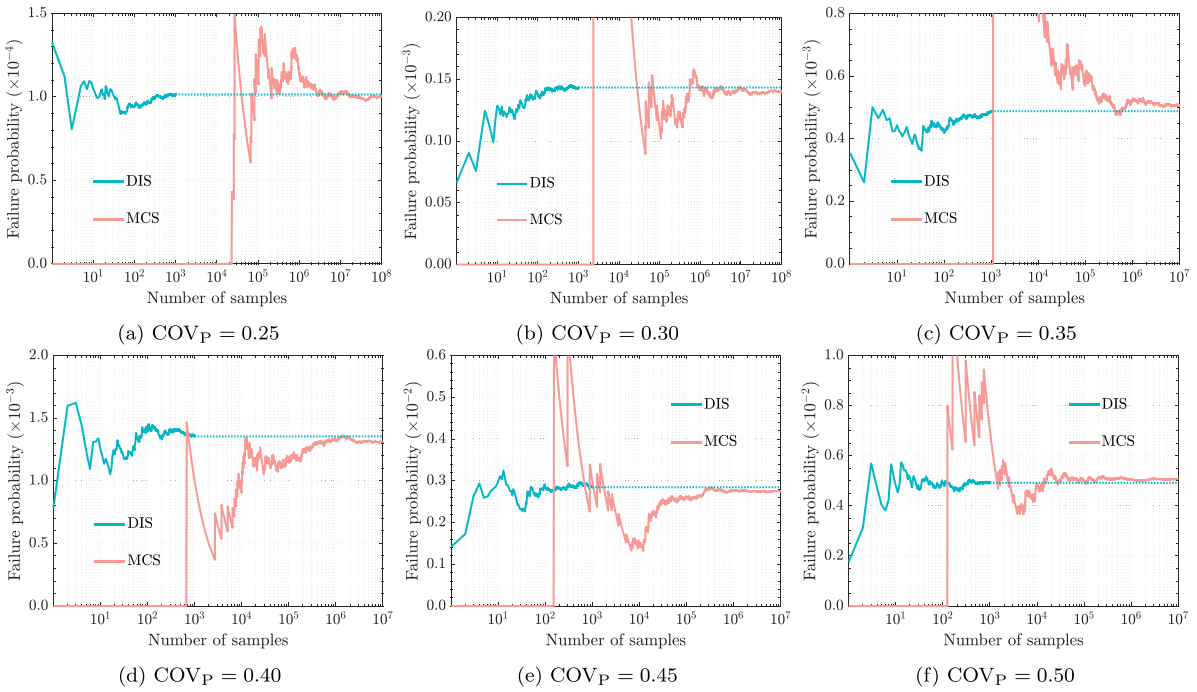

Fig. 8. Failure probability with different COV_P for example 1.

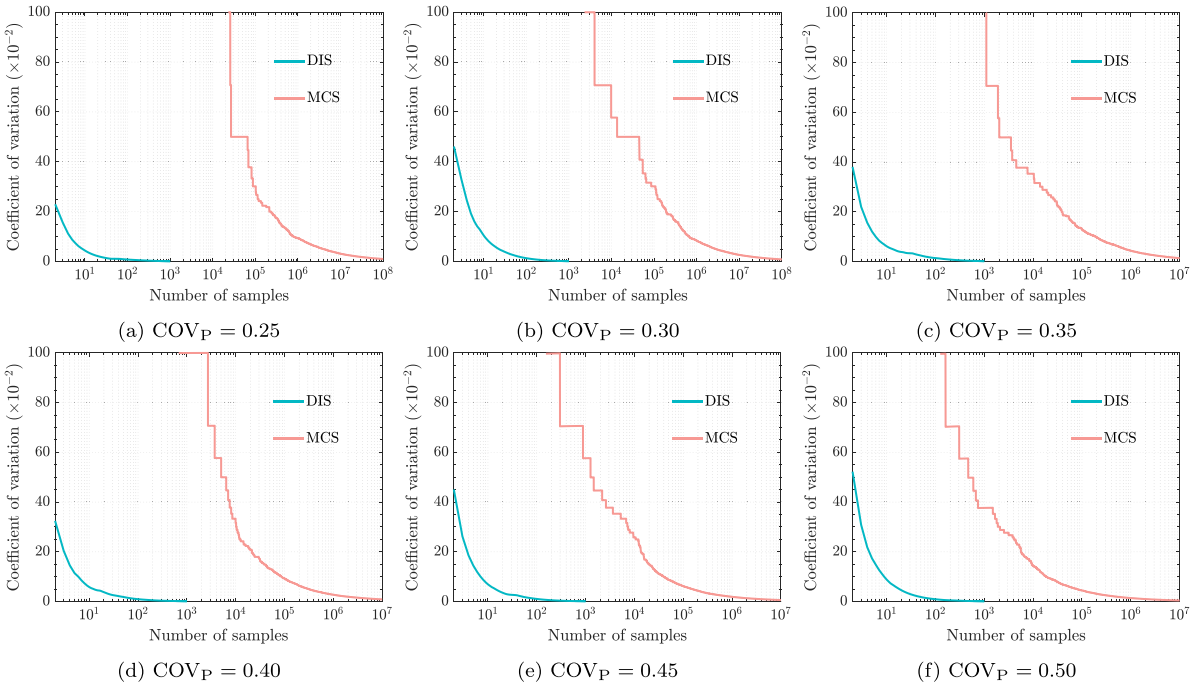

Fig. 9. Coefficient of variation of failure probabilities with different COV_P for example 1.

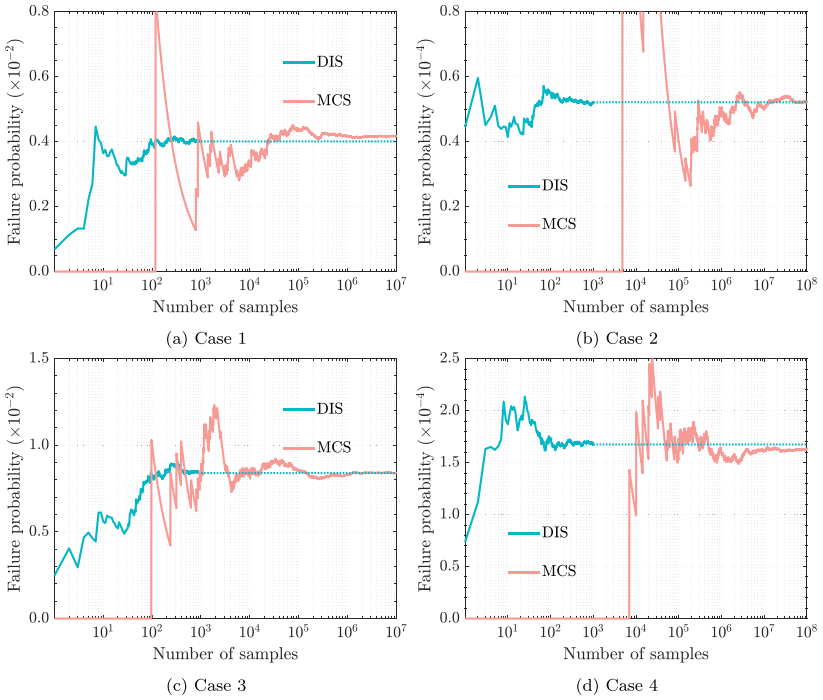

Fig. 10. Failure probability with different thresholds for example 1.

5.1.3. *Influence of failure probability*

To investigate the influence of failure probability on the performance of developed DIS method, the dynamic reliability analysis is conducted for weakly non-Gaussian cases with redefined thresholds. The cases under consideration are as follows:

- Case 1: $\mathrm{COV_P} = 0.35$, $b_{1,1} = 4.5$ m and $b_{1,2} = -0.75$ m
- Case 2: $\mathrm{COV_P} = 0.35$, $b_{1,1} = 7.5$ m and $b_{1,2} = -1.25$ m
- Case 3: $\mathrm{COV_P} = 0.40$, $b_{1,1} = 4.5$ m and $b_{1,2} = -0.75$ m
- Case 4: $\mathrm{COV_P} = 0.40$, $b_{1,1} = 7.5$ m and $b_{1,2} = -1.25$ m

The failure probabilities obtained from the developed DIS method and MCS are compared in Figs. 10(a)–10(d), along with the COVs of estimated failure probabilities compared in Figs. 11(a)–11(d). The results demonstrate that the failure probabilities obtained using the developed DIS method closely align with those from MCS, underscoring the accuracy of the DIS method across various levels of failure probability. Moreover, the developed DIS method achieves stability with fewer than 1000 samples across various cases, underscoring its precision for scenarios with low failure probabilities in the level of 10^{-5}.

5.1.4. *Influence of distribution type*

To further investigate the influence of distribution type on the performance of the developed DIS method, the excitation is assumed to follow different types of distribution, including normal, Weibull, Gamma, and Uniform distributions. Again, the failure probability is estimated using the developed DIS method and MCS, and the results are compared in Figs. 12(a)–12(d). The COVs of failure probability obtained by using different methods are compared in Figs. 13(a)–13(d).

It can be seen that, the developed DIS method can reach a stable evaluation using about 1000 samples. And the failure probability obtained from the developed DIS method is in close agreement with that from MCS with more than 10^6 samples. These results show the flexibility of the developed DIS method for commonly used non-Gaussian distributions. Specifically, when the load follows Gaussian distribution, there is no assumption in the sample generation procedure. Furthermore, the failure probabilities for loads following different distributions vary, even when they have the same COV. This highlights the necessity of considering the influence of non-Gaussianity.

5.2. *Example 2: two-degree-of-freedom oscillator*

The second example focuses on a two-story shear beam model as shown in Fig. 14. The mass, lateral stiffness and classical damping of two floors are assumed to be the same with the values given as: $m_1 = m_2 = 3 \times 10^4$ kg, $k_1 = k_2 = 18 \times 10^6$ N/m and $d_1 = d_2 = 4\%$. The structure is subject to a force that is modeled by non-Gaussian white noise with COV = 0.35. The discrete white

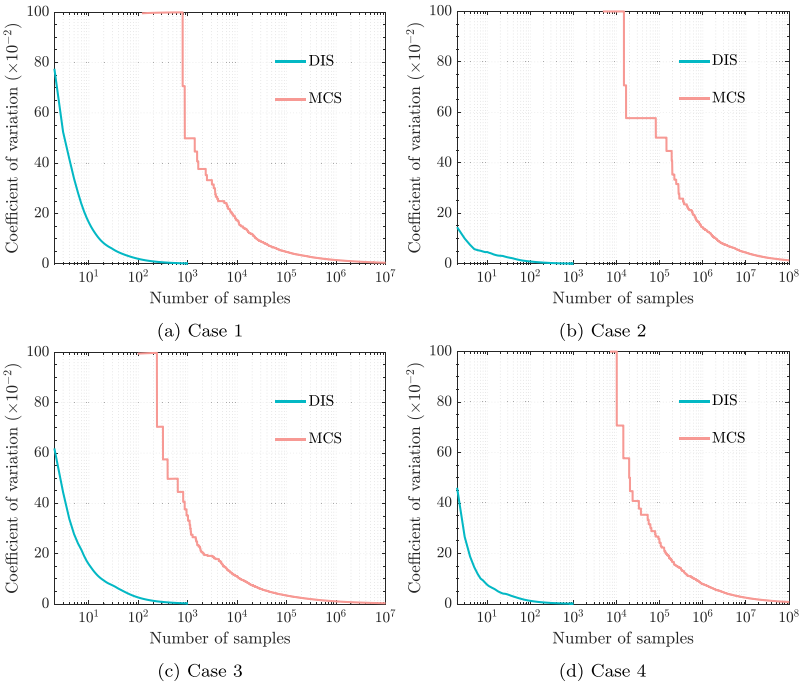

Fig. 11. Coefficient of variation of failure probabilities with different thresholds for example 1.

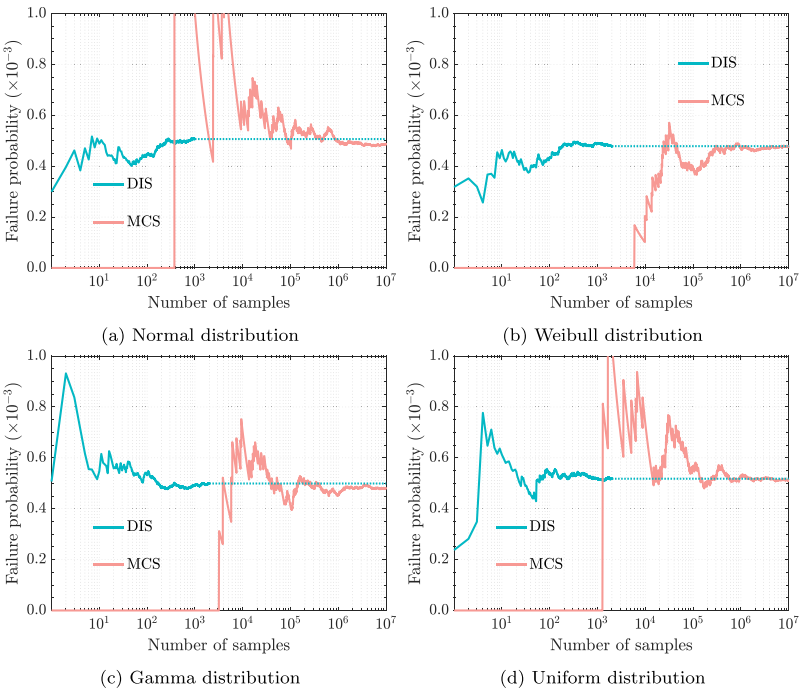

Fig. 12. Failure probability with the load following different distributions for example 1.

noise process possesses a spectral intensity $S = 1 \times 10^{-4}\,\mathrm{m^2/s^3}$, a duration of $T = 15$ s and is represented considering a time step $\Delta t = 0.01$ s. The responses of interest include the relative displacements of the first and second floors relative to the ground, as well as the interstory displacement. Consistently, the thresholds for all these responses are identical, and denoted as b_1 and b_2 for upper and lower excursions, respectively.

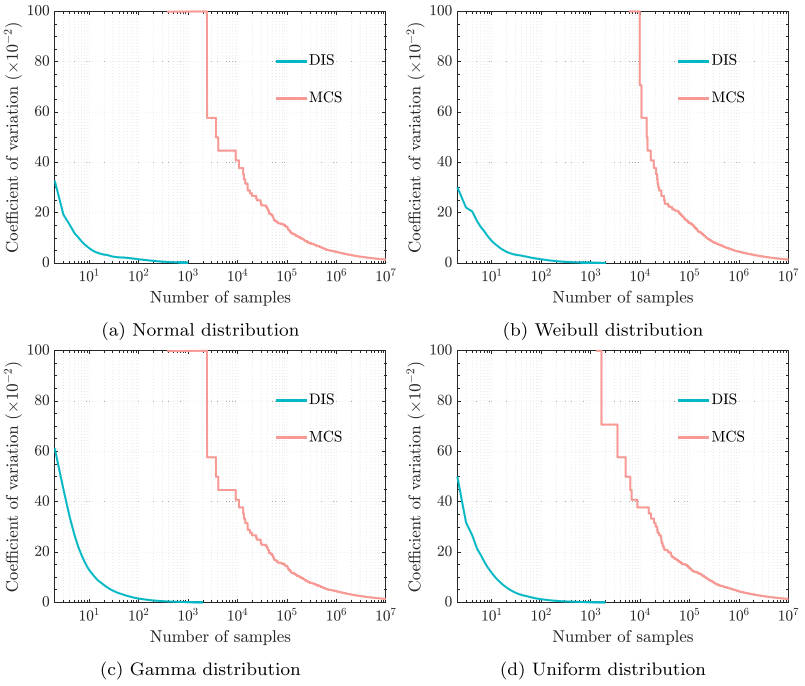

Fig. 13. Coefficient of variation of failure probabilities with the load following different distributions.

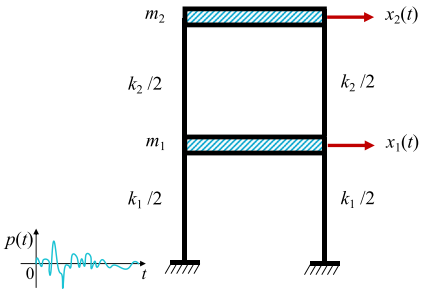

Fig. 14. Schematic graph of two-story shear beam model in example 2.

Six cases are considered with different distribution types for loads and thresholds as follows:

- Case 1: $p(t)$ follows lognormal distribution with $b_1 = 0.008$ m and $b_2 = -0.0018$ m
- Case 2: $p(t)$ follows Gamma distribution with $b_1 = 0.008$ m and $b_2 = -0.0072$ m
- Case 3: $p(t)$ follows Weibull distribution with $b_1 = 0.008$ m and $b_2 = -0.0072$ m
- Case 4: $p(t)$ follows lognormal distribution with $b_1 = 0.0088$ m and $b_2 = -0.008$ m
- Case 5: $p(t)$ follows Gamma distribution with $b_1 = 0.0088$ m and $b_2 = -0.008$ m
- Case 6: $p(t)$ follows Weibull distribution with $b_1 = 0.0088$ m and $b_2 = -0.008$ m

The loads is modulated by function $m(t)$ as follows:

$$m(t) = \begin{cases} (t/5)^2 & 0 \text{ [s]} \le t \le 5 \text{ [s]} \\ 1 & 5 \text{ [s]} < t \le 6 \text{ [s]} \\ e^{-(t-6)^2} & t > 6 \text{ [s]} \end{cases} \tag{57}$$

For each of the case described above, the failure probability and its associated coefficient of variation are calculated by the developed DIS method with 1000 samples and MCS with more than 10^7 samples, and the results are compared in Figs. 15(a)–16(f). The failure probabilities obtained using the developed DIS method remain in close agreement with those from MCS, with the level of failure probability reaching 10^{-5}. Furthermore, the developed DIS method becomes stable with around 1000 samples for all the cases considered. The results demonstrate that the developed DIS method can provide stable estimator for small failure probability.

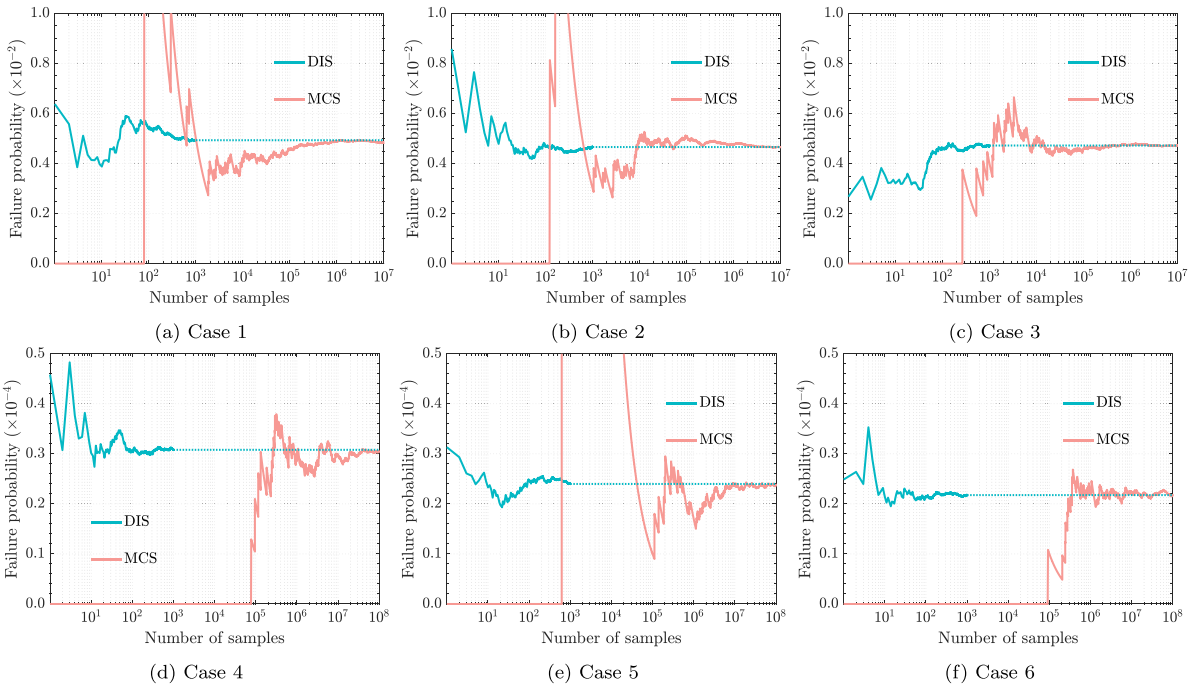

Fig. 15. Failure probabilities for different cases in example 2.

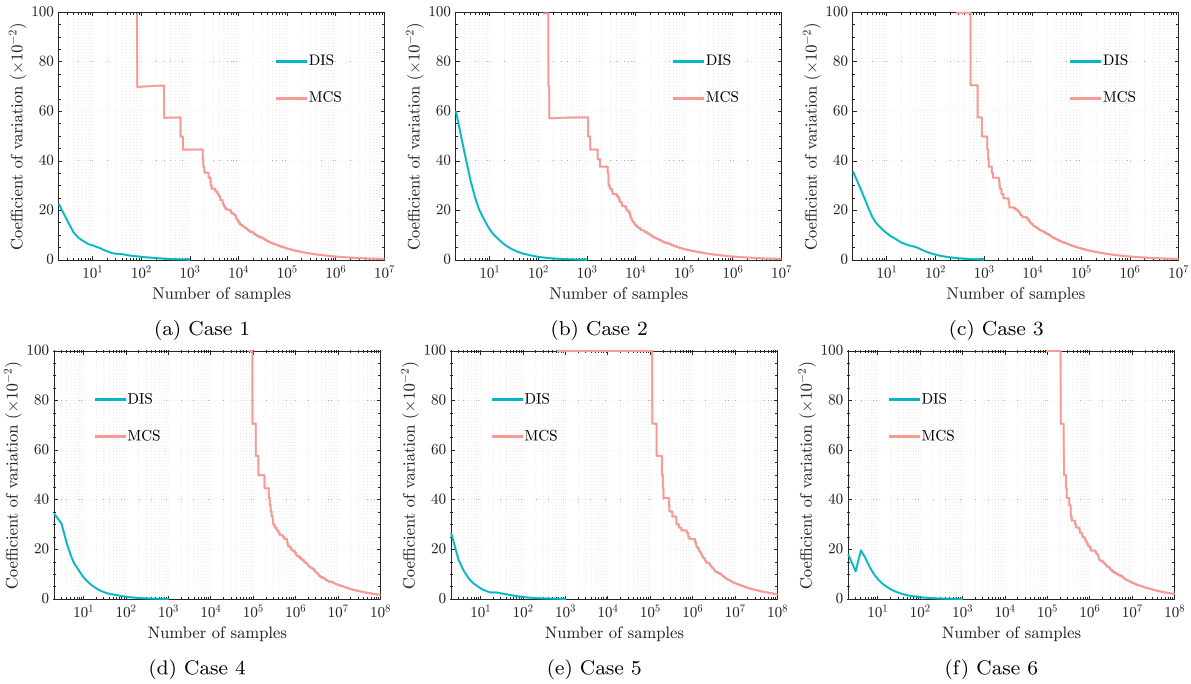

Fig. 16. Coefficient of variation of failure probabilities for different cases in example 2.

To further evaluate the efficiency of the developed DIS method for dynamic reliability analysis, the number of dynamic structural analyses required by the DIS method and the MCS method are compared in Figs. 17(a)–17(f). Dashed lines are used to extend the results of the DIS method, facilitating a clear comparison. It is evident from the figures that the total number of dynamic analyses required by the developed DIS method is significantly less than that required by the MCS method. This reduction is due to the smaller number of random samples needed in the DIS method. However, when the number of samples is the same for both

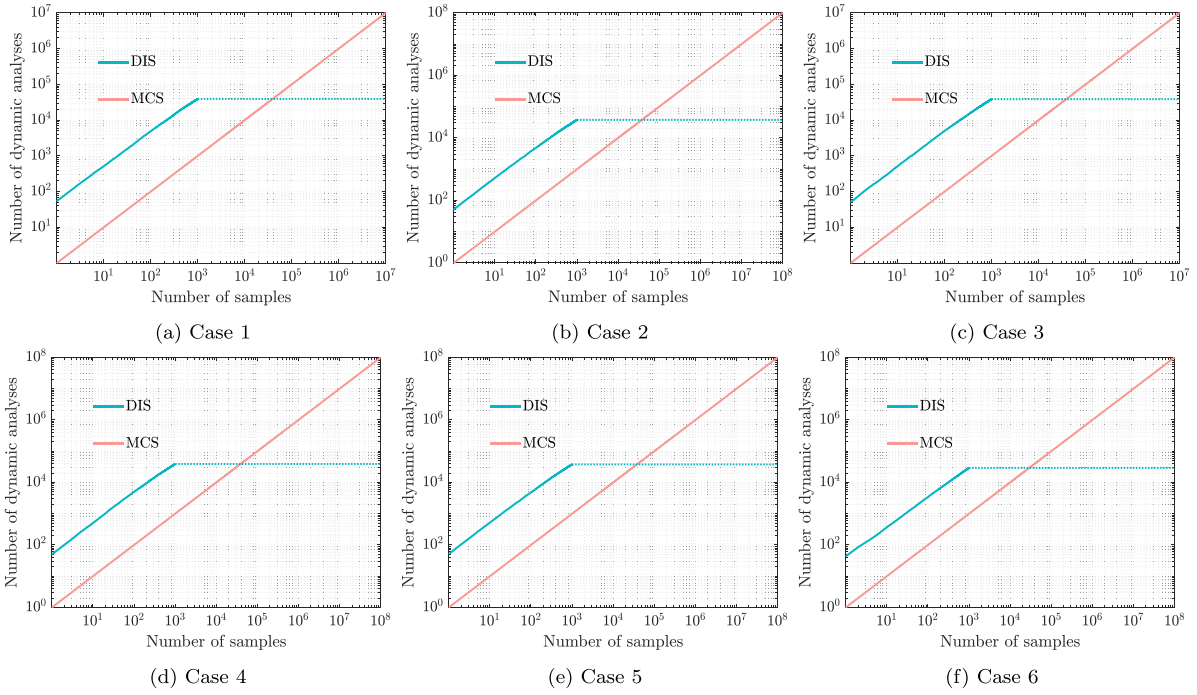

Fig. 17. Number of dynamic structural analyses for different cases in example 2.

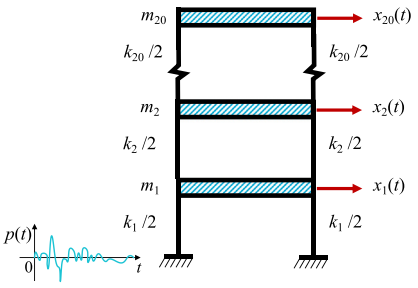

Fig. 18. Schematic graph of multiple story shear beam model in example 1.

methods, the dynamic analyses required by the DIS method exceed those of the MCS method. This is because the developed DIS method necessitates the evaluation of the elementary failure probabilities, the search for the design point, the determination of the intersection point between the limit states of elementary failure events, and the generated direction.

5.3. Example 3: Multiple degree-of-freedom oscillator

The third example involves a 20-story shear frame model, as illustrated in Fig. 18. Each floor has a mass of $m_i = 1 \times 10^5$ kg and nominal stiffness of $k_i = 140 \times 10^6$ N/m, with $i = 1, \ldots, n$, where n is the number of storeys. The frame is subject to a ground acceleration $p(t)$ over a time duration of $T = 20$ s, modeled as Gamma white noise with a COV of 0.20 and a spectral intensity of 10^{-4} m^2/s^3. The stochastic action $p(t)$ is represented by discretized white noise, $\mathbf{p}$, with a time step of $\Delta t = 0.01$ s. The response of interest of this model is the interstorey displacements. The thresholds for all responses are identical, with upper and lower excursion limits denoted as $b_1 = 0.35$ mm and $b_2 = -3.5$ cm, respectively.

The failure probabilities obtained from the developed DIS method with 2000 samples is compared with that from crude MCS in Fig. 19(a), and the corresponding COV of the estimated failure probabilities are compared in Fig. 19(b). To facilitate direct comparison, dashed lines are used to extend the DIS results in Fig. 19(a). It is demonstrated that the failure probabilities estimated by the DIS method are in close agreement with those from MCS, indicating the accuracy of the DIS method for multiple degrees-of-freedom problems. It should be noted that to achieve a COV below 5%, more than 1000 samples are required by the DIS method for

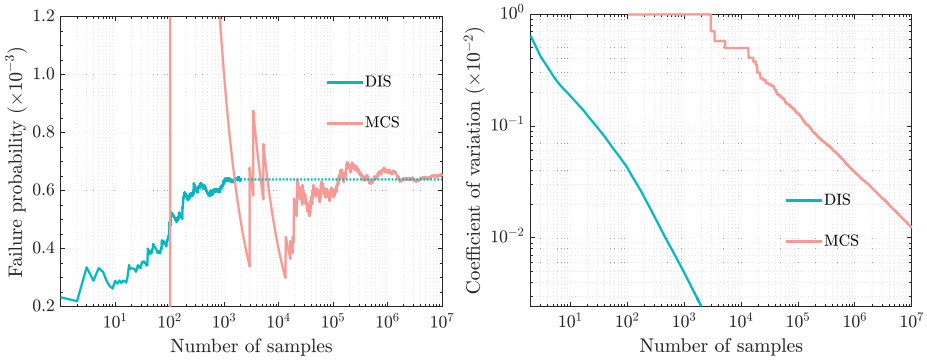

(a) Failure probability (b) COV of failure probability

Fig. 19. Dynamic reliability results in example 3.

this 20-story shear frame model. The computational time required by the DIS method and MCS is 1288 s and 22,232 s, respectively. All scripts were coded in MATLAB R2023b and run on a computer with a 13th Gen Intel(R) Core(TM) i7-1360P @2.20 GHz, while parallel implementation is applied in MCS to improve the efficiency. The ratio of computational time for MCS relative to the developed DIS method is smaller than the ratio of samples required by the two methods. This is because the DIS method incurs additional computational time for generating directional vector samples and parallelization was not applied. However, it should be noted that eventually, parallelization strategies for DIS could be developed.

6. Conclusions

The DIS method is developed for linear structural system subjected to non-Gaussian white noise excitation. An explicit estimator of failure probability is deduced, taking the advantages of both linearity of limit state in physical space and statistical character of Gaussian space. Failure samples are generated in Gaussian space and transformed to physical space. The direction vector in physical space is defined based on failure samples, and the failure probability along the generated direction is calculated with a linear assumption of the normal and inverse normal transformation.

Three examples are investigated to examine the application of the developed DIS method, with the loads following different kinds of non-Gaussian distributions. The developed DIS method is found to be applicable for weakly non-Gaussian white noise excitations with enough precision (measured in terms of a small coefficient of variation) and a reduced number of samples. Specifically, the developed DIS method remains efficient for small failure probability problem, with about 1000 samples required for problems with a failure probability in the level of 10^{-5}. It should be noted that, due to the assumption of linearity along sampled directions when transforming from the physical space to the standard normal space, the proposed DIS method may not be accurate for estimating the failure probability for excitations that exhibit strong non-Gaussianity or deviate from white noise.

CRediT authorship contribution statement

Xuan-Yi Zhang: Writing – review & editing, Writing – original draft, Validation, Methodology, Conceptualization. **Mauricio A. Misraji:** Writing – review & editing, Methodology. **Marcos A. Valdebenito:** Writing – review & editing, Validation, Supervision, Conceptualization. **Matthias G.R. Faes:** Writing – review & editing, Supervision, Project administration, Funding acquisition, Conceptualization.

Declaration of competing interest

The authors declare the following financial interests/personal relationships which may be considered as potential competing interests: Matthias G.R. Faes reports financial support was provided by Alexander von Humboldt Foundation. If there are other authors, they declare that they have no known competing financial interests or personal relationships that could have appeared to influence the work reported in this paper.

Acknowledgments

The study is partially supported by the National Natural Science Foundation of China (Grant Nos.:52108104), the Alexander von Humboldt Foundation, Germany for the postdoctoral grant of Xuan-Yi Zhang, and the Henriette Herz Scouting program, Germany (Matthias G.R. Faes). The authors gratefully acknowledge the supports.

Appendix. Hasofer–Lind–Rackwitz–Fiessler algorithm for searching design point

The design point corresponding to $G_{U,i,s}(t_k,\mathbf{u})$, i.e., $\mathbf{u}^*_{i,k,s}$, is the point on the LSF $G_{U,i,s}(t_k,\mathbf{u})=0$ that is closest to the origin in the standard normal space. The search for $\mathbf{u}^*_{i,k,s}$ involves solving the following optimization problem:

$$\min_{\mathbf{u}} \|\mathbf{u}\| \quad \text{subject to} \quad G_{U,i,s}(t_k,\mathbf{u})=0. \tag{A.1}$$

This problem can be solved using iterative methods such as the Hasofer–Lind–Rackwitz–Fiessler (HLRF) algorithm [44], and the iterative steps are summarized as follows:

(1) **Initialization**: Start with an initial guess $\mathbf{u}^{(0)}$. Generally, $\mathbf{u}^{(0)}$ is set to be a zero vector.

(2) **Iteration**: Update the design point using the following equations until convergence.

$$\mathbf{u}^{(j+1)}=\mathbf{u}^{(j)}-\frac{G_{U,i,s}(t_k,\mathbf{u}^{(j)})}{\|\nabla G_{U,i,s}(t_k,\mathbf{u}^{(j)})\|^2}\nabla G_{U,i,s}(t_k,\mathbf{u}^{(j)}), \tag{A.2}$$

where $\nabla G_{U,i,s}(t_k,\mathbf{u})$ is the gradient of the LSF with respect to $\mathbf{u}$. Considering the chain rule for differentiation, $\nabla G_{U,i,s}(t_k,\mathbf{u})$ is calculated as follows:

$$\nabla G_{U,i,s}(t_k,\mathbf{u}^{(j)})=\nabla G_{i,s}(t_k,\mathbf{p}^{(j)})\frac{d\mathbf{p}}{d\mathbf{u}}\bigg|_{\mathbf{p}=\mathbf{p}^{(j)}}. \tag{A.3}$$

Recall $f_{\mathbf{P}}(\mathbf{p})d\mathbf{p}=\phi_{\mathbf{U}}(\mathbf{u})d(\mathbf{u})$ and use the definition of $G_{i,s}(t_k,\mathbf{p}^{(j)})$ given in Eq. (10), $\nabla G_{U,i,s}(t_k,\mathbf{u})$ can be reformulated as follows:

$$\nabla G_{U,i,s}(t_k,\mathbf{u}^{(j)})=(-1)^{(s+1)}\mathbf{h}_i(t_k)\mathbf{J}, \tag{A.4}$$

where $\mathbf{J}$ is the Jacobian matrix, which in this case is a diagonal matrix whose elements are given by $\phi_{\mathbf{U}}(\mathbf{u}^{(j)})\oslash f_{\mathbf{P}}(\mathbf{p}^{(j)})$, where $\oslash$ denotes Hadamard division.

(3) **Convergence Check**: The iteration stops when the change in $\mathbf{u}$ is smaller than a predefined tolerance ζ, i.e., $\|\mathbf{u}^{(j+1)}-\mathbf{u}^{(j)}\|<\zeta$.

Data availability

Data will be made available on request.

References

[1] S.H. Crandall, First-crossing probabilities of the linear oscillator, J. Sound Vib. 12 (3) (1970) 285–299.
[2] Stephen O. Rice, Mathematical analysis of random noise, Bell Syst. Tech. J. 23 (3) (1944) 282–332.
[3] B.F. Spencer Jr., I. Elishakoff, Reliability of uncertain linear and nonlinear systems, J. Eng. Mech. 114 (1) (1988) 135–148.
[4] Jie Li, Jianbing Chen, Stochastic Dynamics of Structures, John Wiley & Sons, 2009.
[5] Dan Wang, Jie Li, An efficient load effect combination method based on probability density evolution method, Struct. Saf. 97 (2022) 102217.
[6] Harald Cramér, On the intersections between the trajectories of a normal stationary stochastic process and a high level, Arkiv Mat. 6 (4–5) (1966) 337–349.
[7] Erik H. Vanmarcke, Properties of spectral moments with applications to random vibration, J. Eng. Mech. Div. 98 (2) (1972) 425–446.
[8] Ram Gopal Bhandari, R.E. Sherrer, Random vibrations in discrete nonlinear dynamic systems, J. Mech. Eng. Sci. 10 (2) (1968) 168–174.
[9] M.F. Dimentberg, An exact solution to a certain non-linear random vibration problem, Int. J. Non-Linear Mech. 17 (4) (1982) 231–236.
[10] Tong Zhou, Yongbo Peng, Reliability analysis using adaptive polynomial-chaos kriging and probability density evolution method, Reliab. Eng. Syst. Saf. 220 (2022) 108283.
[11] Tong Zhou, Yongbo Peng, Jie Li, An efficient reliability method combining adaptive global metamodel and probability density evolution method, Mech. Syst. Signal Process. 131 (2019) 592–616.
[12] Cheng Su, Baomu Li, Taicong Chen, Xihua Dai, Stochastic optimal design of nonlinear viscous dampers for large-scale structures subjected to non-stationary seismic excitations based on dimension-reduced explicit method, Eng. Struct. 175 (2018) 217–230.
[13] Zhiyuan Xia, Ser Tong Quek, Aiqun Li, Jianhui Li, Maojun Duan, Hybrid approach to seismic reliability assessment of engineering structures, Eng. Struct. 153 (2017) 665–673.
[14] Anders M.J. Olsson, Göran E. Sandberg, Latin hypercube sampling for stochastic finite element analysis, J. Eng. Mech. 128 (1) (2002) 121–125.
[15] Michael D. Shields, Jiaxin Zhang, The generalization of latin hypercube sampling, Reliab. Eng. Syst. Saf. 148 (2016) 96–108.
[16] Siu-Kui Au, James L. Beck, Estimation of small failure probabilities in high dimensions by subset simulation, Probab. Eng. Mech. 16 (4) (2001) 263–277.
[17] Jianye Ching, Siu-Kui Au, James L. Beck, Reliability estimation for dynamical systems subject to stochastic excitation using subset simulation with splitting, Comput. Methods Appl. Mech. Engrg. 194 (12–16) (2005) 1557–1579.
[18] Mahdi Norouzi, Efstratios Nikolaidis, Integrating subset simulation with probabilistic re-analysis to estimate reliability of dynamic systems, Struct. Multidiscip. Optim. 48 (2013) 533–548.
[19] S.K. Au, J.L. Beck, First excursion probabilities for linear systems by very efficient importance sampling, Probab. Eng. Mech. 16 (3) (2001) 193–207.
[20] Iason Papaioannou, Sebastian Geyer, Daniel Straub, Improved cross entropy-based importance sampling with a flexible mixture model, Reliab. Eng. Syst. Saf. 191 (2019) 106564.
[21] Sebastian Geyer, Iason Papaioannou, Daniel Straub, Cross entropy-based importance sampling using Gaussian densities revisited, Struct. Saf. 76 (2019) 15–27.
[22] Phaedon-Stelios Koutsourelakis, Helmuth J Pradlwarter, Gerhart Iwo Schuëller, Reliability of structures in high dimensions, part I: algorithms and applications, Probab. Eng. Mech. 19 (4) (2004) 409–417.
[23] Xiaodong Zhang, Ying Min Low, Chan Ghee Koh, Maximum entropy distribution with fractional moments for reliability analysis, Struct. Saf. 83 (2020) 101904.

[24] Lambros Katafygiotis, Sai Hung Cheung, Domain decomposition method for calculating the failure probability of linear dynamic systems subjected to Gaussian stochastic loads, J. Eng. Mech. 132 (5) (2006) 475–486.
[25] O. Ditlevsen, P. Bjerager, R. Olesen, A.M. Hasofer, Directional simulation in Gaussian processes, Probab. Eng. Mech. 3 (4) (1988) 207–217.
[26] M.A. Misraji, M.A. Valdebenito, H.A. Jensen, C.F. Mayorga, Application of directional importance sampling for estimation of first excursion probabilities of linear structural systems subject to stochastic Gaussian loading, Mech. Syst. Signal Process. 139 (2020) 106621.
[27] Klaus Jürgen Bathe, Finite Element Procedures, Prentice Hall Englewood Cliffs, NJ, 1996.
[28] Steven F. Wojtkiewicz, Erik A. Johnson, Lawrence A. Bergman, Mircea Grigoriu, Billie F. Spencer Jr., Response of stochastic dynamical systems driven by additive gaussian and poisson white noise: solution of a forward generalized kolmogorov equation by a spectral finite difference method, Comput. Methods Appl. Mech. Eng. 168 (1-4) (1999) 73–89.
[29] Antonina Pirrotta, Multiplicative cases from additive cases: extension of kolmogorov–feller equation to parametric poisson white noise processes, Probab. Eng. Mech. 22 (2) (2007) 127–135.
[30] A Di Matteo, M Di Paola, A Pirrotta, Probabilistic characterization of nonlinear systems under poisson white noise via complex fractional moments, Nonlinear Dyn. 77 (2014) 729–738.
[31] Jian-Bing Chen, Meng-Ze Lyu, Probabilistic response determination of high-dimensional nonlinear dynamical systems enforced by parametric multiple poisson white noises, Nonlinear Dyn. (2024) 1–16.
[32] Yan-Gang Zhao, Zhao-Hui Lu, Structural Reliability: Approaches from Perspectives of Statistical Moments, John Wiley & Sons, 2021.
[33] H.A. Jensen, Structural optimization of linear dynamical systems under stochastic excitation: a moving reliability database approach, Comput. Methods Appl. Mech. Eng. 194 (12–16) (2005) 1757–1778.
[34] Richard L. Burden, Numerical Analysis, Brooks/Cole Cengage Learning, 2011.
[35] J. Nie, B.R. Ellingwood, Directional methods for structural reliability analysis, Struct. Saf. 22 (3) (2000) 233–249.
[36] G.I. Schuëller, R. Stix, A critical appraisal of methods to determine failure probabilities, Struct. Saf. 4 (4) (1987) 293–309.
[37] A.H.S. Ang, W.H. Tang, Probability Concepts in Engineering: Emphasis on Applications to Civil and Environmental Engineering, Wiley, 2007.
[38] G.I. Schuëller, H.J. Pradlwarter, Benchmark study on reliability estimation in higher dimensions of structural systems – An overview, Struct. Saf. 29 (2007) 167–182.
[39] Yan-Gang Zhao, Tetsuro Ono, Moment methods for structural reliability, Struct. Saf. 23 (1) (2001) 47–75.
[40] Yan-Gang Zhao, Xuan-Yi Zhang, Zhao-Hui Lu, A flexible distribution and its application in reliability engineering, Reliab. Eng. Syst. Saf. 176 (2018) 1–12.
[41] Yan-Gang Zhao, Xuan-Yi Zhang, Zhao-Hui Lu, Complete monotonic expression of the fourth-moment normal transformation for structural reliability, Comput. Struct. 196 (2018) 186–199.
[42] Xuan-Yi Zhang, Yan-Gang Zhao, Zhao-Hui Lu, Unified Hermite polynomial model and its application in estimating non-Gaussian processes, J. Eng. Mech. 145 (3) (2019) 04019001.
[43] Rüdiger Rackwitz, Bernd Fiessler, Structural reliability under combined random load sequences, Comput. Struct. 9 (5) (1978) 489–494.
[44] Ove Ditlevsen, Henrik O. Madsen, Structural Reliability Methods, Vol. 178, Wiley New York, 1996.